

PV Integration in LV Networks and Capacity Analysis

Maja Muftić Dedović, Samir Avdaković, Adin Memić

Summary — The increasing integration of photovoltaic (PV) systems in low-voltage (LV) networks presents challenges in violation of permitted voltage changes in the LV network and conductor and transformer capacity, which are critical for maintaining grid reliability and operational efficiency. This paper analyzes PV integration, focusing on voltage control, conductor capacity, and the importance of day-ahead PV generation and consumption for proactive grid management. Using MATLAB, the LV network is modeled to assess voltage analysis and conductor capacity for PV capacities ranging from 3 kW to 8 kW per consumer. Predictions of day-ahead PV production are conducted using a feedforward neural network trained on meteorological data such as solar irradiance, temperature, and cloud cover. The predictive model enabled voltage drop simulations and capacity analysis under forecasted conditions. The results demonstrated that voltage levels remained within the permissible range (+5%, -10% of 400 V) for PV capacities up to 8 kW, ensuring operational reliability. The neural network-based predictions are closely aligned with modeled values, with minimal differences, validating the forecasting approach. Voltage variations increased with higher PV capacities, but conductor current levels consistently remained below thermal limits. Incremental PV capacity integration revealed the network's ability to support distributed generation effectively but with limitations at higher capacities. This research highlights the role of accurate forecasting and optimization in ensuring reliable renewable energy adoption.

Keywords — Distributed Energy Resources (DERs), Low-Voltage Networks, Neural Networks, Optimization, Prosumers, Voltage Analysis.

I. INTRODUCTION

The increasing penetration of distributed energy resources (DERs), particularly photovoltaic (PV) systems, poses significant challenges and opportunities for modern power distribution networks. With the emergence of prosumers, entities capable of both consuming and producing electricity, and energy communities, the dynamics of energy generation, consumption, and grid interaction are rapidly evolving. Efficiently managing these interactions is critical to ensuring grid stability, optimizing energy utilization, and supporting the transition towards sustainable energy systems.

(Corresponding author: Maja Muftić Dedović)

Maja Muftić Dedović, Samir Avdaković, and Adin Memić are with the Faculty of Electrical Engineering, University of Sarajevo, Sarajevo, Bosnia and Herzegovina (e-mails: maja.muftic-dedovic@etf.unsa.ba, samir.avdakovic@etf.unsa.ba, adin.memic@etf.unsa.ba)

Reference [1] address these challenges by proposing a distributed congestion management scheme based on iterative distribution locational marginal pricing (iDLMP). Their approach optimizes prosumer energy operations to alleviate congestion in distribution networks. By considering prosumers as self-organizing units capable of integrating diverse resource flexibilities their scheme enhances local energy sharing and supports the efficient integration of DERs. Incorporating such innovative congestion management strategies is crucial for improving hosting capacities and ensuring stable operation of low-voltage (LV) networks with high DER penetration. Building upon these insights, this research aims to further optimize prosumer integration by addressing voltage regulation challenges and conductor capacity evaluation.

One of the primary challenges associated with PV integration is managing the voltage variations caused by fluctuating energy generation. These fluctuations can lead to voltage drops or rise, potentially exceeding permissible limits and impacting the quality of the power supply. Additionally, the capacity of existing conductors may be insufficient to handle the increased power flow, necessitating careful evaluation to avoid thermal overloads and maintain operational safety.

This paper addresses these challenges by analyzing the effects of PV integration on voltage profiles and conductor capacity in LV networks. The research employs a systematic methodology to evaluate the feasibility of PV integration while ensuring network reliability and compliance with operational standards. The proposed approach includes modeling the network's electrical and geometric characteristics, assessing PV production dynamics, and conducting iterative optimization to identify maximum permissible PV capacities.

The findings of this research aim to provide practical insights for grid operators, policymakers, and engineers in planning and optimizing PV system integration in LV networks, ensuring a balance between renewable energy adoption and system reliability.

A key novelty of this paper is the quantitative evaluation of PV hosting capacity under different penetration scenarios while ensuring compliance with operational voltage limits and conductor thermal ratings. The paper also introduces an iterative assessment methodology that systematically determines the maximum allowable PV capacity in an LV network, offering valuable insights for grid operators and planners.

The comparative analysis of modeled against forecasted PV production demonstrates the reliability of predictive approaches in assessing voltage within permissible limits, reinforcing the importance of proactive grid management. The findings contribute to a more precise estimation of hosting capacity, ensuring efficient integration of renewable energy sources without compromising network reliability.

The key contributions of this paper are as follows.

1. The paper provides a quantitative evaluation of PV hosting capacity in LV networks while ensuring compliance with operational voltage limits and conductor thermal ratings.
2. An iterative assessment methodology is introduced to determine the maximum allowable PV penetration under different scenarios, offering practical insights for grid operators and planners.
3. The research validates the accuracy of predictive models by comparing modeled and forecasted PV generation, ensuring that voltage levels remain within permissible limits.
4. Realistic daily and seasonal load variations are considered, acknowledging their impact on PV integration and network performance.
5. The findings highlight the importance of predictive approaches in optimizing PV integration, facilitating better planning and operational decision-making for LV networks.

This paper is structured as follows. Section II provides a review of relevant literature, highlighting existing research on PV integration in LV networks and identifying key gaps addressed in this research. Section III describes the proposed methodology, including network modeling, PV generation characteristics, and the iterative assessment approach used for hosting capacity evaluation. Section IV presents the implementation of day-ahead PV output prediction using a neural network model, supporting capacity analysis under forecasted conditions. Section V discusses the results obtained from simulations, comparing modeled and forecasted PV production and analyzing voltage and conductor constraints. Finally, Section VI concludes the paper by summarizing key findings and outlining potential directions for future research.

II. LITERATURE REVIEW

Recent advancements in integrating prosumers into power systems emphasize the critical role of digitalization and advanced optimization techniques. Paper [2] explore the strategic behavior of prosumers in electricity markets, demonstrating how DER investments are influenced by market dynamics and proposing regulatory measures to align private and public incentives. Also, [3] introduces a decentralized Virtual Aggregation Environment (VAE), enabling smart prosumers to collaboratively manage flexibility without a central aggregator, highlighting the potential of cooperative-competitive algorithms for enhancing grid reliability. In [4] is employed multi-agent reinforcement learning (MARL) to optimize peer-to-peer energy trading, showing how dynamic pricing mechanisms can improve community self-sufficiency and reduce costs while balancing local supply and demand.

An Internet of Energy (IoE) framework facilitates bidirectional energy transactions and integrates DERs into virtual power plants, with optimization techniques playing a key role in enhancing grid reliability [5]. A stochastic bottom-up model analyzes the effects of PV self-consumption on load profiles, emphasizing the need for detailed prosumer-level modeling to improve forecasting and grid planning [6]. A prosumer-centric peer-to-peer energy trading approach addresses network voltage constraints, balancing social welfare with economic and technical objectives in energy markets [7].

In [8], a hybrid control policy is proposed to address locational disparities in voltage regulation and economic arbitrage, enhancing grid stability and prosumer benefits. The research in [9] focuses on optimizing DER under uncertainty through improved risk management in decision-making models. The research in [10]

examines the impact of distribution tariffs on prosumer demand response, highlighting trade-offs between energy costs and distribution expenses. An incentive-based voltage regulation framework for unbalanced radial networks is developed in [11], balancing prosumer participation and grid needs while reducing operational costs. In [12], an innovative energy management system for LV networks is presented, utilizing prosumer-based ancillary services to manage voltage and reduce congestion.

Challenges such as reverse power flows and voltage fluctuations in LV grids, caused by high penetration of DERs, require advanced grid management tools to improve hosting capacities and maintain stability [13]. A probabilistic approach for maximizing PV hosting capacity through the coordinated management of OLTCs, PV inverters, and EVs demonstrates significant potential for enhancing grid performance and stability [14].

In [15], Prosumer Energy Management Systems (PEMS) are developed to highlight prosumers' dual role as consumers and producers, focusing on advanced communication and optimization techniques for energy sharing and smart grid operations. The research in [16] presents a transactive energy framework using coordinated power control and game theory to optimize prosumer participation, addressing economic incentives and voltage stability. In [17], the financial viability of photovoltaic-battery systems (PV-BSS) is examined, exploring the role of demand response and capacity markets, while identifying challenges related to uncertainty and limited policy support. Reference [18] analyzes the hosting capacity of residential grids with high PV penetration and distributed storage, demonstrating how advanced management systems and coordinated storage utilization mitigate voltage instability and enhance capacity. Finally, [19] reassesses voltage variation strategies, emphasizing that while effective in certain conditions, traditional methods face limitations in achieving substantial energy savings in advanced systems.

Paper [20] explores the role of energy prosumers in sustainable energy transitions, highlighting the socio-economic and policy dimensions of prosumer-driven systems. They underline the need for decentralized configurations and innovative business models to maximize prosumer contributions to net-zero targets. Research in [21] explores energy storage systems (ESS) for active power management and voltage regulation, proposing strategies to maintain grid stability while enhancing prosumer benefits. Also, [22] addresses challenges such as overvoltage and reverse power flow in residential grids with high PV penetration, suggesting scalable battery systems and solar radiation forecasting to ensure voltage stability and energy quality.

Recent research highlights the need to shift from deterministic to stochastic methods for hosting capacity (HC) estimation. Deterministic approaches, though simpler, often overlook the complexities of variable renewable generation and load uncertainties. Stochastic models, such as those in [23], incorporate these uncertainties using advanced optimization techniques, improving accuracy and efficiency over traditional methods. Similarly, [24] demonstrates the limitations of deterministic frameworks and validates the advantages of stochastic approaches in managing PV penetration. Further advancements in HC, as discussed in [25], focus on ESS and dynamic hosting capacity (DHC) strategies, which address voltage rise and reverse power flow issues while enhancing grid reliability through adaptive control and storage integration.

Previous researches on PV hosting capacity have primarily focused on deterministic methods that evaluate network constraints under fixed operating conditions. Unlike these researches, this paper presents a comprehensive approach that integrates both voltage regulation and conductor thermal constraints while systematically determining the maximum feasible PV penetration using an iterative evaluation method. In addition, a comparative analysis

between modeled and forecasted PV generation ensures that the methodology aligns with real-world operational conditions.

III. METODOLOGY

This paper explores the effects of integrating PV systems into LV distribution networks, emphasizing voltage analysis and conductor capacity evaluation. The proposed methodology provides a systematic approach for assessing the feasibility of PV integration while maintaining network reliability. In Figure 1, the algorithm is presented as a flowchart illustrating the applied approach.

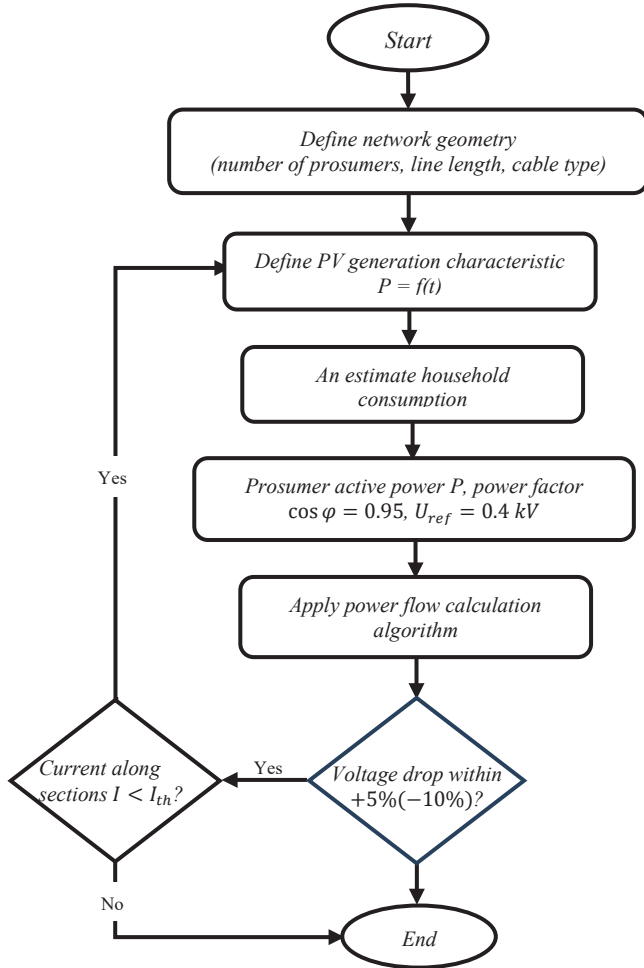


Fig. 1. Flowchart of the applied approach.

A. NETWORK DEFINITION

The geometry of the LV network is characterized by defining the number of consumers or prosumers, the length of distribution lines, and the type of cables used. The length of the cables and their material properties directly influence the resistance and impedance, which are crucial for calculating voltage variations and power losses.

The LV distribution network in this research is modeled with a focus on its electrical and geometric characteristics, including conductor specifications, supply network parameters, transformer details, and load distribution.

The LV network utilizes XP00-A type conductors with a cross-sectional area of $4 \times 70 \text{ mm}^2$. The electrical characteristics of these conductors include a phase resistance of $0.443 \Omega/\text{km}$, a phase reactance of $0.075 \Omega/\text{km}$, a zero-sequence resistance of $1.772 \Omega/\text{km}$, and a zero-sequence reactance of $0.225 \Omega/\text{km}$. The continuous current-carrying capacity of the conductors is 192A. These parameters directly influence the impedance of the network and, consequently, the voltage profile and power losses.

The LV network is fed by a medium-voltage (MV) network operating at a nominal voltage of 10kV, with a short-circuit power of 250MVA and an impedance ratio (R/X) of 0.1. The transformer linking the MV and LV networks is rated at 160 kVA and operates with a primary voltage of 10kV and a secondary voltage of 0.4 kV. Its short-circuit voltage is 4%, and its copper and iron losses are 2.35 kW and 0.46 kW, respectively. The no-load current is 2.3 A, with impedance ratios (Ro/Rt) of 2.0 and (Xo/Xt) of 1.0.

The LV network's nominal voltage is 0.4 kV, with a permissible voltage limit of +5% (-10%) under normal operation conditions. The network primarily serves residential consumers. The diversity factor for a large number of households is set at 0.17, and the typical power factor is 0.95. These parameters represent a realistic load profile for residential areas. A total of 10 consumers are observed on one segment of the low-voltage distribution (cable).

The network's design includes evenly distributed nodes along the outgoing feeder, with specific distances between them. The distances between successive nodes vary, including segments of 0.05 km, 0.025 km, and 0.075 km. These variations reflect the actual spatial distribution of connections in residential neighborhoods and are crucial for calculation of voltage changes and current flows. The cumulative impedance of the network is determined by summing the impedance contributions of these individual segments. This arrangement ensures an accurate representation of real-world network conditions, enabling precise modeling and analysis of voltage profiles and conductor utilization.

B. DEFINING PV CHARACTERISTICS

The production of PV is modeled as a time-dependent function, $P=f(t)$, which accounts for the variation in solar irradiance throughout the day. This function includes factors such as the geographical location, orientation of the panels, and meteorological conditions, all of which impact the energy output of the PV system. A time-series simulation is employed to capture daily and seasonal fluctuations in PV generation, ensuring accurate modeling of the system's behavior.

In addition to PV generation variability, household electricity consumption exhibits daily and seasonal fluctuations, which can influence voltage profiles and network constraints. Higher electricity demand during peak evening hours or winter months may lead to increased voltage drops and higher conductor loading, potentially affecting the network's ability to accommodate additional PV capacity. Conversely, lower demand during midday hours, when PV generation is at its peak, may contribute to higher voltage rise, especially in low-load scenarios.

To ensure a realistic assessment of PV hosting capacity, the methodology considers representative daily load profiles. However, incorporating stochastic load modeling in future research could provide a more detailed evaluation of how dynamic consumption patterns interact with PV generation, allowing for more accurate grid planning and adaptive voltage regulation strategies.

The analysis of electricity production from PV systems is conducted for installed capacities ranging from 3 kW to 8 kW in increments of 1 kW. The simulation is performed using a mathematical model that tracks changes in solar radiation intensity throughout the day, taking into account local climatic and geographical conditions characteristic of regions with a temperate climate. Ideal conditions for a clear day are simulated, with solar radiation intensity peaking at midday. It is assumed that the

panels are installed on a roof with an optimal orientation. These parameters enabled the creation of a daily production profile that follows a typical solar radiation curve.

For a PV system with a capacity of 6 kW, the electricity production over 24 hours, expressed in kilowatts (kW), is shown in Figure 2.b). The production and consumption refer to June 21st, the longest day of the year, also known as the summer solstice.

For higher-capacity systems, such as an 8 kW system, the production curve retains a similar daily pattern, but peak values are proportionally higher. The simulation is carried out under standard test conditions with a maximum irradiance of 1000 W/m² and a panel temperature of 25°C. The production values are validated by comparison with reference data from the literature and standardized simulations for PV systems in similar climatic regions [26,27].

Figure 2. presents the hourly variation of electricity consumption, PV production, and net power demand over a 24-hour for a 6 kW PV system per consumer.

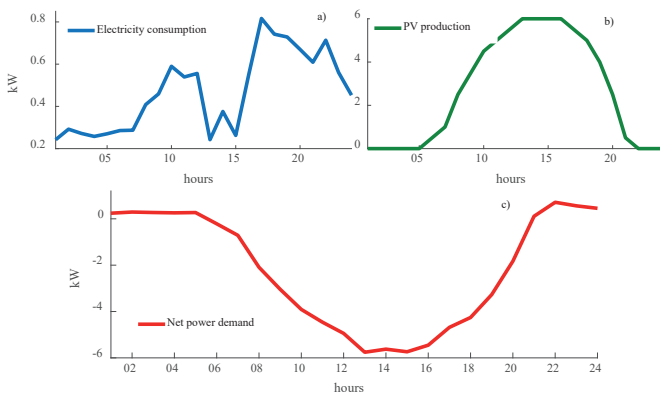


Fig. 2. a.) Electricity consumption, b.) PV Production, and c.) Net power demand over 24 hours for 6 kW.

C. CALCULATION OF POWER DEMAND

For the analysis, household electricity consumption data is calculated over a 24-hour period. The estimated load curve for the year 2024, sourced from the official documents of Public Enterprise Electric Utility of Bosnia and Herzegovina [28], is used as the basis. This curve is multiplied by the average monthly electricity consumption per household in Bosnia and Herzegovina, which is approximately 325 kWh (for June) [29]. The average monthly consumption is calculated by dividing the annual consumption by 12, providing a representative value for analysis. The data is calculated hourly, with each entry representing the average power consumption in kW during one hour. The collected data reflects the dynamics of daily consumption, including variations caused by daily activities, the use of household appliances, and external factors such as temperature and user habits. The collected data is visualized through time series (Figure 2.b)), illustrating changes in consumption throughout the day and enabling the identification of peak loads and periods of reduced consumption.

The net power demand of households (P_D) is determined by subtracting the power supplied by PV panels (P_{PV}) from the household's total power requirements (P_{total}). This relationship is expressed as:

$$P_D = P_{total} - P_{PV} \quad (1)$$

where:

P_D : The net power demand from the distribution network,

P_{total} : The household's internal power demand,

P_{PV} : The power generated by the PV system.

Negative values in the calculated power demand (Figure 2.c)) and Figure 3.) indicate instances where the PV system produced more energy than the household consumption, potentially leading to energy export or storage opportunities. This net power demand is subsequently used to calculate hourly voltage variations across each segment of the distribution network, providing insights into the system's operational stability and efficiency under varying load conditions.

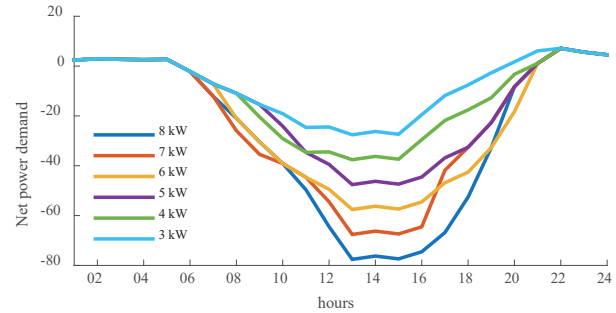


Fig. 3. Net power demand over a 24-hour for PV production from 3 kW to 8 kW.

D. REFERENCE VALUES

For all nodes in the network, the following reference values are used:

- Nominal Voltage: $U_{ref}=400$ V, representing the base operating voltage of the LV network,
- Power Factor: $\cos\phi = 0.95$, reflecting typical power factor values in residential networks.

These values are essential for ensuring that calculations align with the standard operational parameters of the network.

E. VOLTAGE ANALYSIS

An algorithm is implemented to calculate the voltage across all network segments. The algorithm iteratively evaluates whether the voltage at each node remains within +5% (-10%) of the reference voltage (U_{ref}). Voltage drops exceeding this range indicate that corrective measures, such as upgrading cables or redistributing loads, are necessary.

The voltage drop (ΔU) along a segment is calculated using the following formula:

$$\Delta U = I \cdot Z \quad (2)$$

where:

I: The current through the segment,

Z: The impedance of the cable.

Impedance is determined based on the cable's length, cross-sectional area, and material properties.

The mathematical model is presented through the following expressions, which define the power flow calculations in the network based on fundamental electrical relationships.

The reactive power at node i is calculated based on the active power and power factor using the following equation:

$$Q(i) = P(i) \cdot \tan(\varphi) \quad (3)$$

where:

$\cos \varphi$: Power factor at the given node.

$P(i)$: The active power at the given node.

$Q(i)$: The reactive power at the given node.

To determine the voltage drop, the total active and reactive power at node i must be defined as the sum of all preceding nodes in the network:

$$P_{\text{total}}(i) = \sum_{j=1}^n P(j) \quad (4)$$

$$Q_{\text{total}}(i) = \sum_{j=1}^n Q(j) \quad (5)$$

The overall phase angle of the system is determined using the ratio of total reactive power to total active power:

$$\tan \varphi_{\text{total}}(i) = \frac{Q_{\text{total}}(i)}{P_{\text{total}}(i)} \quad (6)$$

where:

P_{total} : Total active power at node i .

Q_{total} : Total reactive power at node i .

φ_{total} : Total phase angle at node i .

$P(j)$: Active power at node j .

$Q(j)$: Reactive power at node j .

n : Total number of nodes in the network.

The calculation of cable impedance includes the series resistance R and reactance X , considering the total phase angle. Effective impedance of the cable directly influences the voltage drop in the network:

$$Z_{\text{aux}} = R + X \cdot \tan \varphi_{\text{total}}(i) \quad (7)$$

The voltage drop along the cable is determined using the following equation:

$$\Delta U = \frac{1000 \cdot P_{\text{total}}(i) \cdot L(i) \cdot Z_{\text{aux}}}{U(i-1)^2} \quad (8)$$

where:

P_{total} : Total active power at node i .

$L(i)$: Length of the cable between nodes $i-1$ and i .

$U(i-1)$: The voltage at the previous node.

The implemented algorithm is illustrated in the following figure, which provides an overview of the steps for calculating voltage drops using MATLAB software [30]. The algorithm iterates over 24 hours, taking into account active and reactive power at each node, total power calculations, and the resulting voltage drop at each segment.

Algorithm 1: Algorithm for Node Voltage Calculation in Distribution Networks

Input: Active power vector P , number of nodes n , \cos_{phi} vector, cable resistances R and reactances X per unit length, cable lengths L , base voltage U_{base} .

Output: Voltage matrix U_{matrix} for all nodes over 24 hours.

```

1 for  $t = 1$  to 24 do
2   Extract active power vector  $P$  for hour  $t$ .
3   Reactive Power and Tangent Phi Calculation:
4   for  $i = 2$  to  $n$  do
5     if  $P(i) == 0$  then
6       Set  $\text{tg\_phi}(i) = 0$ .
7     else
8       Compute reactive power  $Q(i) = P(i) * \tan(\arccos(\cos_{\text{phi}}(i)))$ .
9       Compute  $\text{tg\_phi}(i) = Q(i) / P(i)$ .
10    end
11  end
12  Total Power Calculation:
13  for  $i = 1$  to  $n$  do
14    for  $j = i$  to  $n$  do
15      Accumulate  $P_{\text{total}}(i) += P(j)$ .
16      Accumulate  $Q_{\text{total}}(i) += Q(j)$ .
17    end
18    if  $P_{\text{total}}(i) == 0$  then
19      Set  $\text{tg\_phi}(i) = 0$ .
20    else
21      Compute  $\text{tg\_phi}(i) = Q_{\text{total}}(i) / P_{\text{total}}(i)$ .
22    end
23  end
24  Voltage Drop and Node Voltage Calculation:
25  for  $i = 2$  to  $n$  do
26    Compute auxiliary variable:
27       $Z_{\text{aux}} = R + X \cdot \text{tg\_phi}(i)$ .
28    if  $P_{\text{total}}(i) == 0$  then
29      Set  $\Delta U = 0$ .
30    else
31      Compute voltage drop:
32       $\Delta U = \frac{1000 \cdot P_{\text{total}}(i) \cdot L(i) \cdot Z_{\text{aux}}}{U(i-1)^2}$ .
33    end
34    Update node voltage:
35     $U(i) = U(i-1) - \Delta U \cdot U(i-1)$ .
36  end
37  Store  $U$  in  $U_{\text{matrix}}$  for hour  $t$ .
38 end
39 Output:
40 Return  $U_{\text{matrix}}$ .

```

F. CONDUCTOR CAPACITY VERIFICATION

The current flowing through each network segment is evaluated to ensure it does not exceed the continuous current-carrying capacity (I_{th}) of the cable. For this study, the threshold is set to $I_{\text{th}} = 192\text{A}$.

The verification process involves:

1. **Determining Cable Specifications:** Cable specifications, including the permissible current-carrying capacity under steady-state conditions, are obtained from manufacturer data or relevant standards. Factors such as ambient temperature, installation method, and cable insulation are considered.
2. **Calculating Current Flow:** The current through each segment is calculated as:

$$I = P / (\sqrt{3} \cdot V \cdot \cos\phi). \quad (9)$$

where:

P: Power flow through the segment,

U: Voltage level,

$\cos\phi$: Power factor.

3. **Comparison with Capacity:** The calculated current is compared to I_{th} . If $I > I_{th}$, the cable is insufficient, and recommendations for upgrading are provided.

This verification ensures the thermal safety of the conductors and prevents overloading, which could lead to insulation failure or fire hazards.

G. ITERATIVE OPTIMIZATION PROCESS

An iterative process is applied to optimize the integration of PV. If both voltage and current limits are within acceptable ranges, the installed PV capacity is incrementally increased by 1 kW from 3 to 8 kW. This process continues until one or more constraints are violated, marking the maximum permissible PV capacity for the network. If constraints are exceeded at the initial stage, the analysis concludes with recommendations for network reinforcement or alternative strategies.

The iterative optimization process determines the maximum PV capacity that the network can accommodate while ensuring voltage and current constraints are not violated. The process follows an incremental approach where the PV capacity is increased in steps of $\Delta P = 1$ kW, starting from the initial production $P_{PV,initial}$. The updated PV production at each iteration is given by:

$$P_{PV,new} = P_{PV,prev} + \Delta P \quad (10)$$

At each step, the voltage and current limits are checked:

$$U_{max}(i) < U_{th}, \quad I_{max}(i) < I_{th} \quad (11)$$

where U_{th} and I_{th} represent the permissible voltage and current limits, respectively. If these conditions are met, the iteration continues with an increased PV production. If one or both constraints are exceeded, the process terminates, identifying the maximum allowable PV production for the given network configuration.

IV. DAY-AHEAD PV OUTPUT PREDICTION AND CAPACITY ANALYSIS USING NEURAL NETWORKS

In this section of the paper, a scientific approach is taken to predict day-ahead PV power output and voltage variations on LV networks, as well as to conduct capacity analysis based on PV production data available for the forecasted day. The integration of PV systems into power networks plays a critical role in transitioning towards sustainable energy systems [31]. Accurate

predictions of PV output are essential for optimizing the operation and planning of energy systems, ensuring grid stability, and maximizing the utilization of renewable energy sources, as demonstrated in [32]

The predictive model for PV output utilizes a feedforward neural network (FNN), which is selected for its computational efficiency and ability to capture non-linear relationships between input variables. The model is trained using historical data of PV production and meteorological variables, including solar irradiance, temperature, and cloud cover. These variables are chosen because of their significant impact on PV system performance. The prediction system is developed for six PV systems with nominal capacities ranging from 3 kW to 8 kW.

The neural network architecture includes a single hidden layer with 10 neurons to balance complexity and computational cost. A non-linear activation function, such as sigmoid, is applied in the hidden layer to model complex interactions between inputs, while the output layer employs a linear activation function to produce continuous predictions of PV power output. The Levenberg-Marquardt backpropagation algorithm, a robust optimization method, is used for training. The training process is conducted in MATLAB [30] using the built-in train function.

The input dataset for the neural network consisted of 24 hourly values of PV production for each system, representing typical operational data for one day. Additionally, three key meteorological variables are included: solar irradiance, temperature, and cloud cover. Solar irradiance, measured in watts per square meter (W/m^2), represents the amount of solar energy available to the PV, with values ranging from 0 (night) to $1000 W/m^2$ (peak sunlight). Ambient temperature, measured in degrees Celsius ($^{\circ}C$), affects panel efficiency and ranged from $5^{\circ}C$ in the early morning to $32^{\circ}C$ in the afternoon. Cloud cover, expressed as a percentage, is used to estimate the impact of cloudiness on solar availability, with values ranging from 0% (clear skies) to 100% (fully overcast).

To ensure efficient training and prevent biases caused by scale differences among the input variables, all meteorological inputs are normalized to a range of [0, 1].

The input data matrix X is constructed by combining the hour of the day (1 to 24), normalized solar irradiance, normalized temperature, and normalized cloud cover. The target output matrix Y consisted of historical PV production values for each system.

The neural network is trained using this dataset, with the loss function defined as the mean squared error (MSE) between predicted and actual outputs. The training process iterated for up to 100 epochs or until the model achieved convergence, defined as the minimization of MSE to a predefined threshold.

After training, the model generated day-ahead predictions for each PV system using the same meteorological conditions. These predictions are then utilized for additional analyses, including voltage drop simulations on low-voltage networks and capacity assessments of the PV systems under forecasted conditions.

V. RESULTS AND DISCUSSION

The proposed methodology is tested on an LV distribution network model. The results demonstrated that:

1. Voltage remained within $\pm 5\%$ (-10%) of the nominal voltage for most scenarios.
2. Current levels are below the continuous current-carrying capacity of the cables, ensuring thermal safety.

- Incremental increases in PV capacity allowed for a gradual understanding of the network's limitations.

The results obtained by applying the approach explained in Section III are presented for two cases. The first case utilizes modeled PV production data.

The second case considers forecasted PV production one day ahead, as described in Section IV. Figure 4. illustrates the results for the first case, while Table 1. presents the outcomes for the second case, highlighting the relationship between PV production and voltage levels (U) across various scenarios.

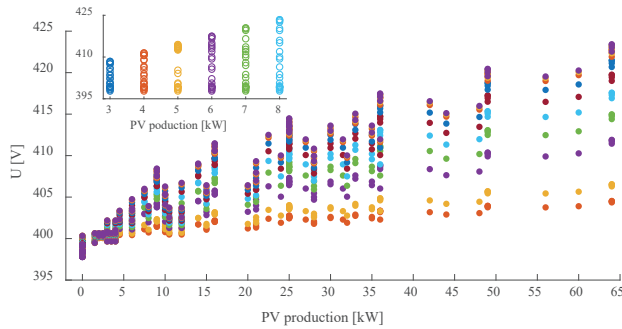


Fig. 4. Relationship between PV production and voltage levels (U) across various scenarios.

TABLE I

COMPARISON OF VOLTAGE (%) FOR MODELED AND FORECASTED PV PRODUCTION AT DIFFERENT POWER LEVELS

PV Production (kW)	Modelled Voltage (%)	Forecasted Voltage (%)	Difference (%)
3	2.11	2.03	0.08
4	2.87	2.92	0.05
5	3.62	3.74	0.12
6	4.37	3.97	0.4
7	5.11	5.25	0.14
8	5.85	5.79	0.06

From the approach provided in section III, it is evident that the voltage levels across the network are significantly influenced by the size of the PV systems, ranging from 3 kW to 8 kW. The voltage levels tend to increase slightly with higher installed PV capacities due to the reverse power flow in scenarios where local generation exceeds demand. For instance, at a PV size of 3 kW, the observed voltage levels are predominantly between 400 V and 405 V, while for larger systems like 8 kW, voltage levels range between 415 V and 420 V. This increase demonstrates that higher PV capacities inject more power into the network, improving voltage profiles but also necessitating careful voltage regulation to avoid overvoltage issues. Crucially, the voltage values for all PV capacities remain within the permissible range of +5% of -10 % of the nominal voltage (400 V), confirming that the LV network is capable of integrating these capacities without breaching operational voltage limits.

The voltage along the network is calculated for a cable length of 500 meters. This length contributes to increased impedance, amplifying voltage variations under higher loads, especially during peak consumption periods. Despite this, the results indicate that the network generally maintains adequate voltage under most conditions. For instance, at a 3 kW PV production level, voltage variations remain minimal, with average below 2 V, demonstrating a well-balanced network response. However, at higher capacities, such as 8 kW, maintaining acceptable voltage levels becomes

more challenging. While the average voltage drop across nodes is approximately 8.5 V, there are instances where the maximum voltage drop exceeds the critical threshold of 20 V. This highlights a potential risk of exceeding acceptable voltage levels at higher levels of distributed generation, particularly under certain load and generation configurations.

The variation in voltage across the network depends on the installed PV production, with higher capacities leading to increased voltage fluctuations. Table II presents the voltage observed in the network for different PV production levels.

TABLE II

VOLTAGE IN THE NETWORK FOR DIFFERENT PV PRODUCTION

PV Production (kW)	Voltage (V)
3	408.44
4	411.48
5	414.49
6	417.48
7	420.46
8	423.42

To address these challenges and ensure reliable network operation, especially in scenarios with higher PV penetration, optimization measures are essential. The integration of ESS, such as batteries, could help mitigate voltage fluctuations by absorbing excess generation during peak production and releasing energy during periods of high demand. Additionally, network interconnectivity and reinforcement, including meshing LV networks or upgrading conductor capacities, could reduce impedance and stabilize voltage profiles.

Furthermore, the implementation of advanced digital solutions, such as real-time monitoring and control systems, would enable timely detection of voltage deviations and facilitate rapid corrective actions. Digitalizing the management of distributed generation through smart inverters and automated demand response could dynamically adjust generation and consumption patterns to maintain voltage within acceptable limits.

These strategies emphasize the importance of a proactive approach to grid management, particularly as PV penetration continues to increase. A combination of optimization, ESS, network upgrades, and digitalization will ensure that acceptable voltage levels are maintained, even under demanding conditions. Such measures are critical for transitioning toward a resilient, sustainable, and future-ready power distribution system.

As PV sizes increase, voltage at the nodes gradually rises, particularly during periods of high solar irradiance, as power is injected into the network. This phenomenon is most evident for systems between 6 kW and 8 kW, where voltage levels at distant nodes are observed to peak around 420 V, compared to closer nodes which maintain voltages near 410 V. Hourly data trends further validate these findings, showing a stable voltage profile across multiple days. During peak production hours, typically midday, the voltage increases across the network are more uniform, whereas during early morning or evening hours, when PV generation is lower, the network operates closer to its base voltage of 400 V.

The results also indicate that the observed current values remain consistently below the maximum permissible limit of 192 A for XP00-A conductors. At peak conditions with an 8 kW PV system, the maximum current observed is approximately 120 A,

providing sufficient headroom for safe operation. Similarly, for lower capacities such as 3 kW, current levels are typically below 50 A, highlighting the efficiency of the network under partial loading conditions. Table III presents the maximum observed current for different PV production, ensuring that all values remain below the permissible thermal limit of 192 A.

TABLE III

MAXIMUM CURRENT IN CONDUCTORS FOR DIFFERENT PV PRODUCTION

PV Production (kW)	Max. Current (A)
3	41.83
4	57.43
5	72.34
6	87.47
7	102.39
8	117.44

Lastly, the analysis of integration capacity demonstrates that incremental increases in PV capacities, from 3 kW to 8 kW, allow the network to integrate distributed generation effectively while maintaining reliability. However, further increases in PV capacity beyond 8 kW may necessitate network reinforcements, such as upgrading conductor cross-sectional areas or transformer capacities, to ensure continued compliance with voltage and current limits.

These results from Table I. demonstrate that the forecasted voltage closely align with the modeled values, with variations remaining within acceptable ranges. However, at higher PV production levels, the voltage drops approach critical thresholds (20 V and above), indicating a potential risk of exceeding acceptable voltage limits.

For a PV production of 3 kW, the modeled voltage drop corresponds to 8.44 V, while the forecasted drop is 8.12 V, with a negligible difference of 0.32 V. At 4 kW, the modeled drop increases to 11.48 V, and the forecasted value closely aligns at 11.68 V, resulting in a minor difference of 0.20 V. Similarly, at 5 kW, the modeled drop is 14.48 V, compared to the forecasted value of 14.96 V, with a difference of 0.48 V.

As the power level increases to 6 kW, the modeled voltage drop is 17.48 V, while the forecasted value is slightly lower at 15.88 V, resulting in a larger difference of 1.60 V. For 7 kW, the modeled and forecasted drops are 20.44 V and 21.00 V, respectively, with a difference of 0.56 V. Finally, at 8 kW, the modeled voltage drop is 23.40 V, and the forecasted value is nearly identical at 23.16 V, showing an excellent match with a minor difference of 0.24 V.

This underscores the importance of implementing measures such as energy storage, enhanced grid interconnectivity, and real-time monitoring to mitigate the impact of high PV penetration on maintaining acceptable voltage levels in the network.

The transformer under consideration has a nominal capacity of 160 kVA, equivalent to approximately 152 kW at a power factor of 0.95, typically feeding a LV network with four outgoing feeders. This analysis focuses on one feeder with 10 connections, where individual loads range from 3 kW to 8 kW, corresponding to feeder loads between 30 kW and 80 kW. This load represents approximately 19.7% to 52.6% of the transformer's total capacity, which is within operational limits, provided the total load across all feeders does not exceed 152 kW. Assuming equal distribution, the nominal load per feeder would be 38 kW, however, one feeder with a load of up to 80 kW would require reduced loads on the remaining feeders

to prevent overloading. Voltage regulation, with a short-circuit voltage of 4%, remains adequate, but high feeder loads, especially with long cable lengths, could result in critical voltage variations. At a power factor of 0.95, the current for an 80 kW load reaches approximately 121 A, requiring careful impedance considerations to maintain voltage compliance within the allowable +5% (-10%) range of 400 V. While copper losses of 2.35 kW and iron losses of 0.46 kW indicate efficient operation under nominal conditions, sustained operation near maximum capacity could increase thermal stress, necessitating adequate cooling and monitoring to prevent insulation degradation. Proper load management and redistribution, along with voltage analysis and future scalability considerations, are essential, particularly if additional PV generation or higher loads are integrated. Incorporating reactive power compensation, monitoring, and automation can enhance operational reliability and prevent system overload.

The proposed methodology provides insights for grid operators in determining the maximum permissible PV hosting capacity in LV networks. However, its implementation in real-world scenarios requires considerations related to cost and complexity. The computational approach used in this paper, based on voltage and conductor capacity verification, can be integrated into existing distribution network planning tools to support decision-making processes. While the methodology itself is straightforward, its practical application may involve additional investments in monitoring infrastructure and advanced control systems to manage higher PV penetration levels effectively. Regulatory support and incentive structures may be required to encourage grid operators to adopt such analytical approaches in routine operations.

In real-world applications, PV generation is influenced by factors such as cloud cover, shading, panel aging, and seasonal variations, leading to deviations from expected production levels. These fluctuations can impact voltage profiles and the overall capacity of PV systems to offset household consumption. Lower-than-expected PV output may reduce the extent of voltage rise but can also limit the benefits of distributed generation in reducing grid dependence.

To account for these uncertainties, future research should explore probabilistic modeling approaches that incorporate variability in solar irradiance and load fluctuations. Integrating real-time monitoring and adaptive control mechanisms could help mitigate the effects of variable PV output, enhancing overall system stability and efficiency.

VI. CONCLUSION

This research analyzed the integration of PV systems into LV networks, focusing on voltage and conductor capacity. Using a systematic approach, the study demonstrated that PV capacities up to 8 kW could be integrated effectively while maintaining voltage levels within the permissible range (+5%, -10% of 400 V) and ensuring that conductor currents remain below thermal limits.

Key findings indicate that:

1. The tested conditions maintain acceptable voltage variations in the LV network, even at higher levels of PV penetration. However, the approach highlights the risk of overvoltage issues in scenarios of peak solar irradiance, particularly for systems exceeding 8 kW capacity.
2. Forecasted PV production values, obtained through neural network-based predictions, closely align with modeled data, showcasing the reliability and accuracy of the predictive model.

To address potential challenges in scenarios with increased PV

penetration, the following recommendations are proposed:

- Incorporation of ESS to absorb excess energy during peak production and release it during periods of high demand, mitigating voltage fluctuations.
- Network upgrades such as increasing conductor cross-sectional areas or upgrading transformers, are critical to support higher PV capacities.
- Implementing real-time monitoring and control systems, including smart inverters and automated demand response, will enhance the dynamic management of voltage and current levels.
- Policymakers and grid operators should adopt iterative and predictive methodologies for network design, ensuring long-term scalability and reliability.

By adopting these strategies, LV networks can support the transition to renewable energy systems while maintaining operational efficiency and stability. Future research should explore dynamic hosting capacity models and integrate stochastic methods to better account for uncertainties in load and generation patterns. This will further enhance the adaptability and resilience of power distribution systems in the face of growing renewable energy integration.

REFERENCES

- [1] Mahmud, K., M. J. Hossain, and G. E. Town, "Peak-load reduction by coordinated response of photovoltaics, battery storage, and electric vehicles," *IEEE Access*, vol. 6, pp. 29353–29365, 2018, doi: 10.1109/ACCESS.2018.2837144
- [2] Siddiqui, A. S., and S. A. Siddiqui, "Ambiguities and nonmonotonicities under prosumer power: Optimal distributed energy resource investment in a deregulated electricity industry," *Top*, vol. 30, no. 3, pp. 492–532, 2022, <https://doi.org/10.1007/s11750-022-00628-2>
- [3] Arnone, D., M. Cacioppo, M. G. Ippolito, M. Mammina, L. Mineo, R. Musca, and G. Zizzo, "A methodology for exploiting smart prosumers' flexibility in a bottom-up aggregation process," *Appl. Sci.*, vol. 12, no. 1, Art. no. 430, 2022, <https://doi.org/10.3390/app12010430>
- [4] May, R., and P. Huang, "A multi-agent reinforcement learning approach for investigating and optimising peer-to-peer prosumer energy markets," *Appl. Energy*, vol. 334, Art. no. 120705, 2023, <https://doi.org/10.1016/j.apenergy.2023.120705>
- [5] Mahmud, K., B. Khan, J. Ravishankar, A. Ahmadi, and P. Siano, "An internet of energy framework with distributed energy resources, prosumers and small-scale virtual power plants: An overview," *Renew. Sustain. Energy Rev.*, vol. 127, Art. no. 109840, 2020, <https://doi.org/10.1016/j.rser.2020.109840>
- [6] Karalus, S., B. Köpfer, P. Guthke, S. Killinger, and E. Lorenz, "Analysing grid-level effects of photovoltaic self-consumption using a stochastic bottom-up model of prosumer systems," *Energies*, vol. 16, no. 7, Art. no. 3059, 2023, <https://doi.org/10.3390/en16073059>
- [7] Umer, K., Q. Huang, M. Khorasany, W. Amin, and M. Afzal, "A novel prosumer-centric approach for social welfare maximization considering network voltage constraints in peer-to-peer energy markets," *Int. J. Electr. Power Energy Syst.*, vol. 147, Art. no. 108820, 2023, <https://doi.org/10.1016/j.ijepes.2022.108820>
- [8] Hashmi, M. U., D. Deka, A. Bušić, and D. Van Hertem, "Can locational disparity of prosumer energy optimization due to inverter rules be limited?," *IEEE Trans. Power Syst.*, vol. 38, no. 6, pp. 5726–5739, 2022, doi:10.1109/TPWRS.2022.3223842
- [9] Choi, S., K. Park, and S.-O. Shim, "Comparing validity of risk measures on newsvendor models in open innovation perspective," *J. Open Innov. Technol. Market Complex.*, vol. 4, no. 1, pp. 1–12, 2018, <https://doi.org/10.1186/s40852-017-0078-8>
- [10] Avau, M., N. Govaerts, and E. Delarue, "Impact of distribution tariffs on prosumer demand response," *Energy Policy*, vol. 151, Art. no. 112116, 2021, <https://doi.org/10.1016/j.enpol.2020.112116>
- [11] Yang, J., M. R. Alam, W. Tushar, and T. K. Saha, "Incentivizing prosumer voltage regulation for unbalanced radial distribution networks," *IEEE Trans. Sustain. Energy*, vol. 15, no. 1, pp. 81–94, 2023, doi: 10.1109/TSTE.2023.3274154
- [12] Wasiak, I., M. Szypowski, P. Kelm, R. Mieński, A. Wędzik, R. Pawelek, M. Małaczek, and P. Urbanek, "Innovative energy management system for low-voltage networks with distributed generation based on prosumers' active participation," *Appl. Energy*, vol. 312, Art. no. 118705, 2022, <https://doi.org/10.1016/j.apenergy.2022.118705>
- [13] Nazari-pouya, H., "Integration and control of distributed renewable energy resources," *Clean Technol.*, vol. 4, no. 1, pp. 149–152, 2022, <https://doi.org/10.3390/cleantechnol4010010>
- [14] Ali, A., K. Mahmoud, and M. Lehtonen, "Maximizing hosting capacity of uncertain photovoltaics by coordinated management of OLTC, VAr sources and stochastic EVs," *Int. J. Electr. Power Energy Syst.*, vol. 127, Art. no. 106627, 2021, <https://doi.org/10.1016/j.ijepes.2020.106627>
- [15] Zafar, R., A. Mahmood, S. Razzaq, W. Ali, U. Naeem, and K. Shehzad, "Prosumer based energy management and sharing in smart grid," *Renew. Sustain. Energy Rev.*, vol. 82, pp. 1675–1684, 2018, <https://doi.org/10.1016/j.rser.2017.07.018>
- [16] Yang, J., W. Tushar, T. K. Saha, M. R. Alam, and Y. Li, "Prosumer-driven voltage regulation via coordinated real and reactive power control," *IEEE Trans. Smart Grid*, vol. 13, no. 2, pp. 1441–1452, 2021, doi: 10.1109/TSG.2021.3125339
- [17] Clastres, C., O. Rebenaque, and P. Jochem, "Provision of demand response by French prosumers with photovoltaic-battery systems in multiple markets," *Energy Syst.*, vol. 14, pp. 869–892, 2023, doi: 10.1007/s12667-021-00482-4.
- [18] Palacios-Garcia, E. J., A. Moreno-Muñoz, I. Santiago, I. M. Moreno-Garcia, and M. I. Milanés-Montero, "PV hosting capacity analysis and enhancement using high resolution stochastic modeling," *Energies*, vol. 10, no. 10, Art. no. 1488, 2017, <https://doi.org/10.3390/en10101488>
- [19] Faranda, R., and H. Hafezi, "Reassessment of voltage variation for load power and energy demand management," *Int. J. Electr. Power Energy Syst.*, vol. 106, pp. 320–326, 2019, <https://doi.org/10.1016/j.ijepes.2018.10.012>
- [20] Hu, J.-L., and M.-Y. Chuang, "The importance of energy prosumers for affordable and clean energy development: A review of the literature from the viewpoints of management and policy," *Energies*, vol. 16, no. 17, Art. no. 6270, 2023, <https://doi.org/10.3390/en16176270>
- [21] Mieński, Rozmysław, Przemysław Urbanek, and Irena Wasiak, "Using energy storage inverters of prosumer installations for voltage control in low-voltage distribution networks," *Energies*, vol. 14, no. 4, Art. no. 1121, 2021, doi: 10.3390/en14041121.
- [22] Torres, Igor Cavalcante, Daniel M. Farias, Andre LL Aquino, and Chiguera Tiba, "Voltage regulation for residential prosumers using a set of scalable power storage," *Energies*, vol. 14, no. 11, Art. no. 3288, 2021, doi: 10.3390/en14113288.
- [23] Koirala, Arpan, Tom Van Acker, Reinilde D'hulst, and Dirk Van Hertem, "Hosting capacity of photovoltaic systems in low voltage distribution systems: A benchmark of deterministic and stochastic approaches," *Renewable Sustainable Energy Rev.*, vol. 155, Art. no. 111899, 2022, <https://doi.org/10.1016/j.rser.2021.111899>
- [24] Koirala, Arpan, Tom Van Acker, Md Umar Hashmi, Reinilde D'hulst, and Dirk Van Hertem, "Chance-constrained optimization based PV hosting capacity calculation using general polynomial chaos," *IEEE Trans. Power Syst.*, vol. 39, no. 1, pp. 2284–2295, 2023, doi: 10.1109/TPWRS.2023.3258550
- [25] Zobaa, Ahmed F., Shady H. E. Abdel Aleem, Sherif M. Ismael, and Paulo F. Ribeiro, eds., *Hosting Capacity for Smart Power Grids*, Berlin, Germany: Springer, 2020.
- [26] J. S. Stein, C. P. Cameron, B. Bourne, A. Kimber, J. Posbic, and T. Jester, "A standardized approach to PV system performance model validation," in 2010 35th IEEE Photovoltaic Specialists Conference, Honolulu, HI, USA, June 2010, pp. 001079–001084, doi: 10.1109/PVSC.2010.5614696
- [27] SMA Solar Technology AG, "Sunny Design," [Online]. Available: <https://www.sunnydesignweb.com/sdweb/#/Home>, Accessed on: Dec. 15, 2024.
- [28] Public Enterprise Electric Utility of Bosnia and Herzegovina. "Documents and Forms," [Online]. Available: <https://www.epbih.ba/eng/page/documents-and-forms>, Accessed on: Dec. 15, 2024.
- [29] Worlddata.info. "Energy consumption in Bosnia and Herzegovina," [Online]. Available: <https://www.worlddata.info/europe/bosnia-and-herzegovina/energy-consumption.php>, Accessed on: Dec. 25, 2024.
- [30] MathWorks, Inc. "MATLAB R2024a," Natick, MA, USA, 2024. [Online]. Available: <https://www.mathworks.com/products/matlab.html>, Accessed on: Dec. 10, 2024.
- [31] M. M. Dedović, S. Avdaković, A. Mujezinović, and N. Dautbašić, "Integration of PV into the Sarajevo Canton energy system—Air quality and heating challenges," *Energies*, vol. 14, p. 123, 2021. [Online]. Available: <https://doi.org/10.3390/en14010123>
- [32] A. Memić, M. Muftić Dedović, N. Dautbašić, and M. Kapo, "Application of neural networks for predicting energy production from hybrid power systems considering the influence of stochastic weather changes," *B&H Electr. Eng.*, vol. 18, no. 2, pp. 11–17, 2024, doi: 10.2478/bheec-2024-0006.